Hyper-sensitive microwave sensor based on split ring resonator (SRR) for glucose measurement in water

Mohamed Amine Zidane, Amar Rouane, Cherif Hamouda, Hichem Amar

Version of Record: https://www.sciencedirect.com/science/article/pii/S0924424721000625
Manuscript_dcf7636b835b6f8f3653a289af0c3047

Hyper-Sensitive Microwave Sensor based on Split Ring Resonator(SRR) for Glucose Measurement in Water

Mohamed Amine ZIDANE[a], Amar Rouane[a], Cherif Hamouda[b], Hichem Amar[c]

[a] *IJL, CNRS, University of lorraine, Campus ARTEM, 2 allée André Guinier, Nancy, 54500, Meurth-et-moselle, France.*
Tel.: +33755868004
[b] *alciom, 3 Rue des Vignes, Viroflay, 78220, France*
[c] *Center in Industrial Technologies(RCIT), 64 Cheraga, Algiers, 16014, Algeria*

Abstract

A microwave sensor for glucose concentration measurement is presented. The proposed sensor is composed of two cells of circular Split Ring Resonator (SRR) with a liquid holder put on both cells. Those resonators are coupled to a coplanar line forming a two-port network whose S-parameter response provide an information about the dielectric properties of the liquid that is under study. This paper presents a numerical simulation and experimental study of our new configuration of the resonators to assess the sensitivity of the sensor toward small change in glucose concentrations in water. An electronic prototype has been used to improve the detection; a resolution of 1.665mmol/l is reached at the frequency 1.9GHz. The obtained results have shown the effectiveness of this new configuration of resonators sensor for non-invasive measurement on the small change in dielectric parameter ε_r. Therefore, the proposed sensor is well fitted for real time measurement, non-destructive, precise, and low cost.

Keywords: Split Ring Resonators, Electromagnetic Sensor, Non-invasive measurement, Microwave Circuit, Glucose

INTRODUCTION

In recent era, microwave technology has been widely used to develop non-destructive sensors for different purposes such as the materials' identification [1–5]. Also, the microwave sensor has many advantages, such as non-invasive, real time and rapid characterization; moreover, it offers a higher adaptability and flexibility compared to the chemical procedures. Any type or amount of chemical component in the liquid under test produce a variation of the complex dielectric permittivity [6], thus, it affects the electromagnetic response of the sensor.

Email addresses: zidane2@univ-lorraine.fr (Mohamed Amine ZIDANE), amar.rouane@univ-lorraine.fr (Amar Rouane), chamouda@alciom.com (Cherif Hamouda), amar.hichem16@yahoo.fr (Hichem Amar)

January 20, 2021

Based on this method, different electromagnetic sensors have been developed for bio-liquids analysis [7, 8], and more specifically for glucose monitoring applications in blood [9–16].

Glucose is an important component for the commercialization of some products like juices or sodas [17] since its effect is crucial for the flavor and texture. Ensuring the glucose level during the production process is an important aspect for the industry. Likewise, glucose is used as a fermentation substrate to produce wines, beers, spirits, in which it plays an essential role [18]. Chemical method exists but it requires a certain amount of liquid to be extracted for the production process, and hence to be wasted. Repeating this process leads to considerable economic loss, it is why a non-destructive sensor can preserve the sample and avoid losses.

In this paper, we investigate the use of two cells of split ring resonators to characterize the dielectric properties of small samples of liquids and obtain the glucose concentration of different water-glucose solutions at 1.9GHz. Analytical, numerical and experimental studies on SRR (Split Ring Resonator) were presented in [19–24] for their importance in certain applications such as meta materials, detection and dielectric characterization of a material whether solid or fluid [9, 25–33]. This last application is the subject of our study. SRRs are key elements for good detection efficiency in pharmaceuticals and biomedical applications [15]. This is because SRRs have a very high-quality factor, greater than 1000 [34], their miniaturized circular or rectangular shape allows the use of PCB technology for their manufacture. The method, used for the detection in the change of the dielectric parameters such as the permittivity, is based on the influence of the dielectric on the resonant frequency shift. This frequency shift can be quantified by using the power transmission S21 [14]; furthermore, the impedance matching is affected when the dielectric parameter of the medium which is in contact with the resonator, changes. The impedance matching is quantified by the power reflection S11.

Finally, the evaluation process of the glucose can be labor-intensive and expensive. It is why; a simple electronic prototype is proposed to replace VNA and it is used to improve the sensor sensitivity as well.

The electromagnetic sensor

The change in the level of glucose in the medium affects its dielectric properties, such as its permittivity [6].

The principle of this electromagnetic method is based on the near-field radiation generated by the sensor. The study used a fringing electric field, which may be electrically modeled as a capacitor to interfere with the study medium. Therefore, the equivalent input impedance of the sensor in contact with the medium will be affected.

Fig. 1 depicts an illustration of the sensor in contact with water; the sensor consists of a substrate separating the resonators from the coplanar line.

The entire sensor surface was exploited to interact with the medium being studied; for this, four circular SRRs and smaller triangular SRRs were used. The circular and triangular resonators operate at different resonance frequencies. In the proposed configuration, circular SRRs are used for operating at a frequency of 2.1GHz, and the inclusion of triangular

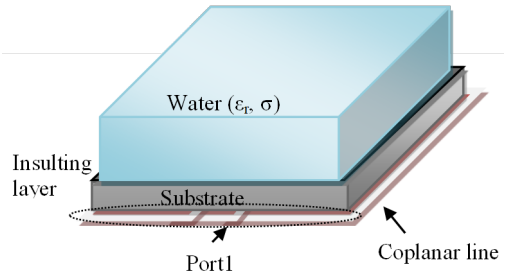

Figure 1: Illustration of the water contact with the sensor

resonators on the substrate surface decrease the operating frequency. This is efficient in improving detection and miniaturizing the sensor.

The wave propagation in the coplanar line is a quasi-TEM mode, which is characterized by an alternating current along the central strip and an alternating magnetic field around the central strip. Then, an induced current is generated on each SRR due to the alternating magnetic field component in the nearby SRR. Noticeably, there exist two kinds of energy in the SRR, including the magnetic energy in the ring and the energy in the split.

The effect of glucose in water will be studied using the designed antenna structure described below. A vector network analyzer (VNA) will be used to validate the experimental studies and to choose an optimal frequency, then an electronic prototype is proposed to improve the sensitivity.

This electromagnetic simulation was performed by designing a coplanar line to provide circular resonators with an outer radius of up to 5.1 mm using magnetic coupling. Therefore, to allow feeding of the resonators, it is important that the width of the middle strip in the coplanar line be twice as large as the outer radius of the ring resonator. Furthermore, the slot dimensions of the coplanar line must be considered due to its effects on the distribution of the electromagnetic fields surrounding the transmission line. However, the coplanar line is considered lossless and its dimensions are calculated using an online calculator to achieve a characteristic impedance of 50Ω. This value is the reference impedance of the coaxial cable. Then resonators, operating at a frequency of 2.1GHz, are included on the second side of the substrate. In comparison, with the micro strip, CPW confines electromagnetic fields in a more limited manner, thereby reducing spurious coupling, radiation, and dispersion. Finally, The magnetic power supply was chosen because the constant relative permeability μ of water is equal to 1 for any change in glucose concentration.

Sensor modeling

The magnitude of S_{11} is defined by Eq. (1):

$$S_{11} = 20log \left| \frac{Z_{in} - Z_0}{Z_{in} - Z_0} \right| \tag{1}$$

Where Z_0 is the characteristic impedance of the coaxial cable, which is equal to 50Ω, and Z_{in} is the input impedance seen at port 1 of the structure. (see figure 3)

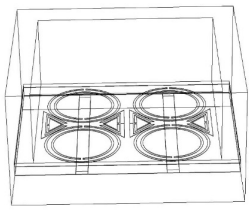

Figure 2: 3D Model of resonators extracted from Comsol®

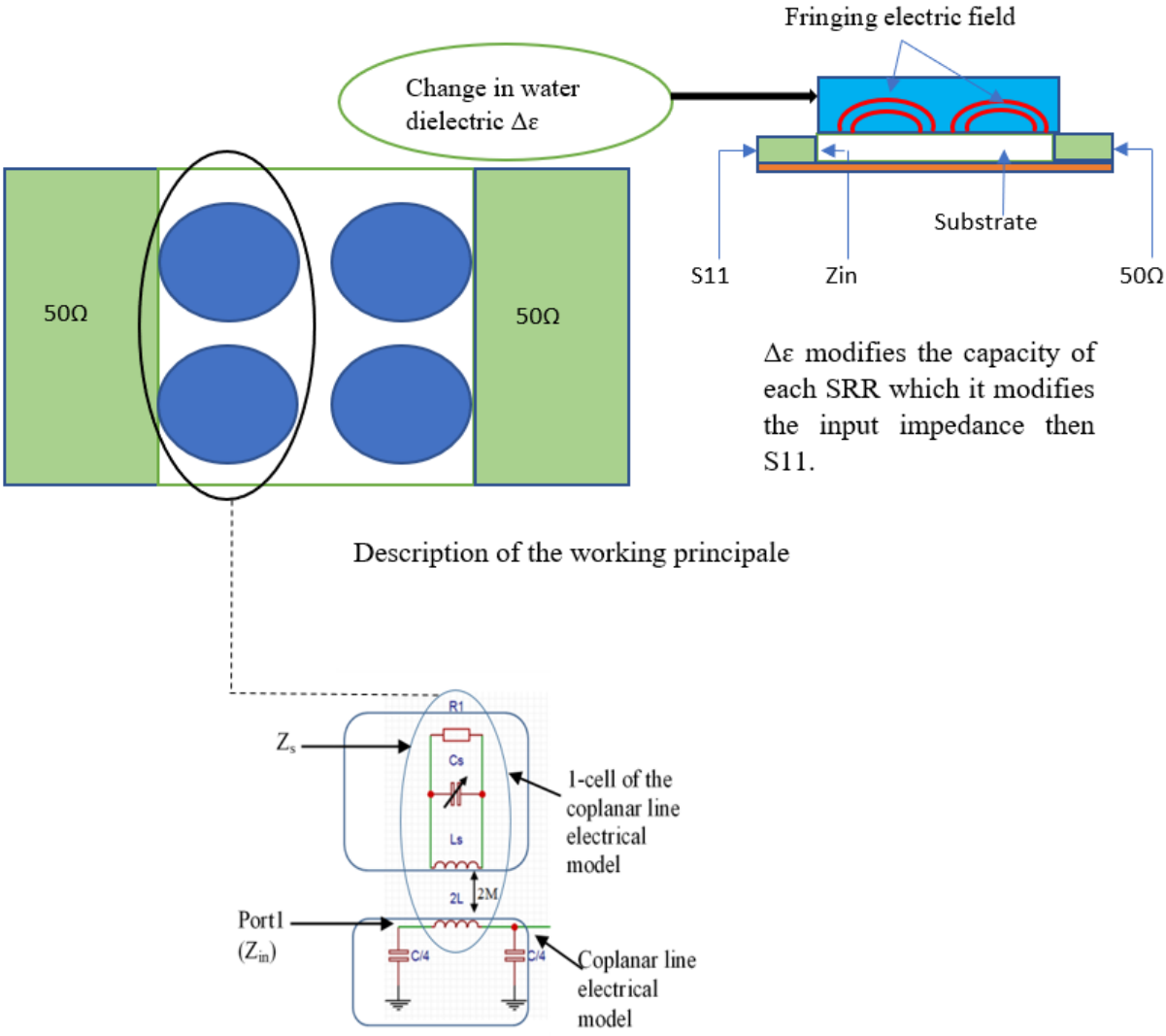

Figure 3: The simplified equivalent circuit of 1-cell of the sensor prototype [24].

Z_s is estimated by Eq (2) [24] :

$$Z_s(\omega, \varepsilon_{eff}) = j\omega L + j\omega^3 \times \left\{ \frac{C_s(\varepsilon_{eff}) M^2 \times \left(1 - \frac{\omega^2}{\omega_0^2}\right) + 2\omega^2 M^2 M' C_s(\varepsilon_{eff})^2}{\left(1 - \frac{\omega^2}{\omega_0^2}\right)^2 - \omega^4 M'^2 C_s(\varepsilon_{eff})^2} \right\} \quad (2)$$

All circular resonators have the same resonance frequency and can be electrically modeled using a lumped element $R_1L_sC_s$, where L_s represents the equivalent inductance of an SRR, considering the mutual inductance between triangular and circular resonators and the mutual inductance between two adjacent circular resonators M' [24]. C_s models an equivalent capacitance considering all the capacitance created between the spires, as well as the capacitance created between the triangular resonators and the circular resonators. By adding a triangular SRR in close proximity to the circular SRR, the capacitive effect can be increased, thereby improving the interaction between our antenna structure and the medium. By modifying the glucose in the medium, the effective permittivity will change. Cs depends on the effective permittivity; as a consequence, Cs will be modified. Then, the input impedance of the structure seen in port1 will be changed. R_1 represents the equivalent resistance considering the conductivity of water [6] and copper. M represents the mutual coupling between the line and the SRR. L and C are the inductance and capacitance of each unit cell of the line. ω_0 is the resonance frequency of each isolated circular resonator. The goal of this model is not to identify its values (because it is a complex analytical study that should identify some parameters that we cannot control, such as the parasite capacities formed in the substrate, the complexity of the geometry of the structure and the behavior of the medium), but to show the implicit relationship between the detection and the reflection parameter S11. This relationship will be demonstrated through simulation in the next section of this paper.

The conductivity of water represents the medium losses toward the electromagnetic field. By introducing changes in the medium conductivity (not shown), simulations were performed on Cosmol® and a poor-quality factor was discovered for a higher conductivity value.

In this simulation, a Rogers 3210 substrate with a permittivity of 10.2 at 2.1 GHz was used to obtain a miniaturized sensor. The dielectric constant of water depends on the frequency, and its exact value is presented in Fig. 4. The resonator was coated by an insulating layer, which could prevent water from meeting the copper in the resonant cavity. The layer had a thickness of 0.5 mm and a permittivity of 2.1.

In the simulation model, experimental data on the dielectric properties of water was imported from the ITIS foundation and introduced into the water block simulated by Comsol. The relative permittivity and conductivity have been expressed as polynomial functions in Eq (3) and Eq (4):

$$\varepsilon_r = -10^{-19}.f^2 - 5.10^{-10}.f + 85.379 \quad (3)$$

$$\sigma = -10^{-19}.f^2 + 6.10^{-10}.f - 0.7813 \quad (4)$$

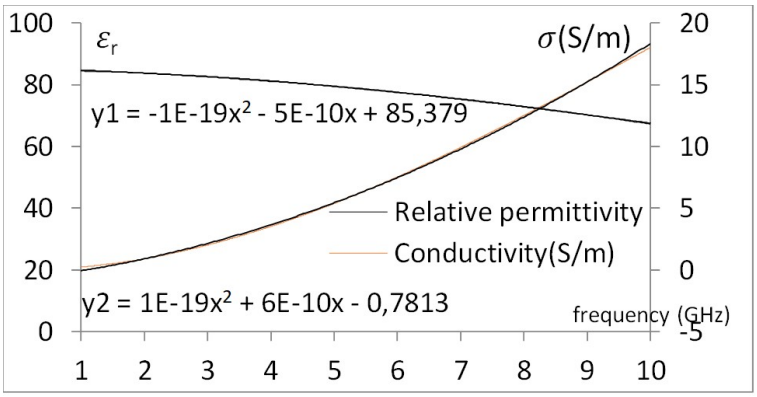

Figure 4: Dielectric constant of water imported from ITIS foundation database [25]

ε_r : represents the relative permittivity of water, σ represents the conductivity (S/m), and f represents the frequency (GHz).

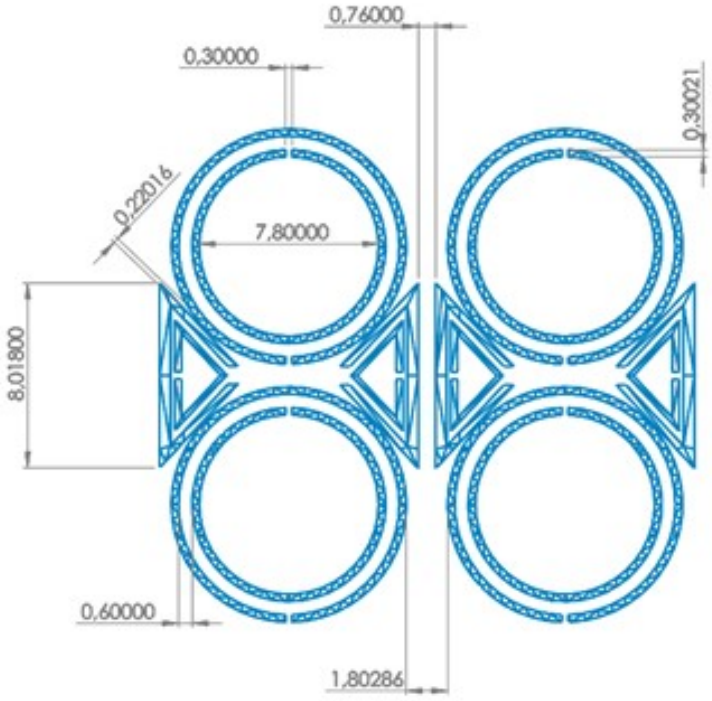

Figure 5: Schematic diagram of the designed sensor. All dimensions are expressed in millimeters.

A variable $\Delta\varepsilon$ has been used in the simulation to represent the incremental step of relative permittivity induced by changes in glucose levels, which is equal to 0.2 [9]. The relative permittivity equation of the water extracted from the curve is increased by the incremental step size $\Delta\varepsilon$ (see Fig. 4). A study on the dielectric properties of the mixture of water and glucose [26] showed that glucose had little effect on the conductivity of water from

1 GHz to 8.5 GHz, and no change was noticed. Based on this study, glucose is considered to have no effect on conductivity. During this simulation, the variation introduced by glucose in the relative permittivity was estimated to be the same around a frequency of 1.88 GHz. The simulation results show that at a fixed frequency, the reflected power increases very slightly due to the increase in the permittivity of mixed water and glucose. This incremental value was chosen to simulate the extremely low glucose concentration in the water, bringing it closer to the presence of glucose in the blood of humans.

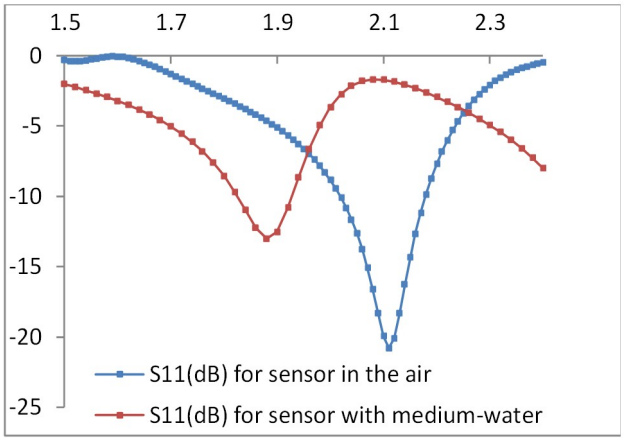

Figure 6: S_{11} vs frequency (GHz)

While placing the simulated water block on the sensor surface, the operating frequency is changed from 2.11GHz to 1.88GHz. Fig. 6 shows that the frequency of the S_{11} peak is decreased by 230 MHz. Fig. 7a presents the S11 vs frequency for different values of water permittivity; the S11 parameter is the reflection coefficient, which is used to indicate the reflected power in port 1 at different frequencies. Different values of the water permittivity simulate different glucose concentrations [35] . A parametric sweep $\Delta\varepsilon$ is used to simulate changes in glucose concentration. The equations (3) and (4) are used to model the dielectric parameter. For our simulation, $\varepsilon r+\Delta\varepsilon$ is used where εr represents the relative permittivity of water, and $\Delta\varepsilon$ is a parameter sweep that varies between 0 and 0.1 in steps of 0.02. This corresponds to 5 different glucose concentrations in water. The results show that an increase in the relative permittivity of water by a step of 0.02 induces a shift of S11 magnitude for different frequencies.

S11 measurements were performed, where port 2 is terminated in a load equal to 50 Ω. the sensor can be used as a stop band filter at the resonance frequency which is not the case of this study. The study frequency range is different from where the stopband filter operates. Indeed, to find the resonance frequency it's simply required to use the transmission parameter S21/dB, which it corresponds to the S21 peak. In our case, the study was conducted with a focus on the frequencies around the peak of S11 and not S21.It should be noted that regardless of the operating frequency, the device generates a fringing electric field at the inter-track level of each SRR. in order to operate the four SRRs in an efficient way, the power transmitted on port 1 must reach all four SRRs, to make this

possible, a work frequency must be selected around the S11/dB peak.

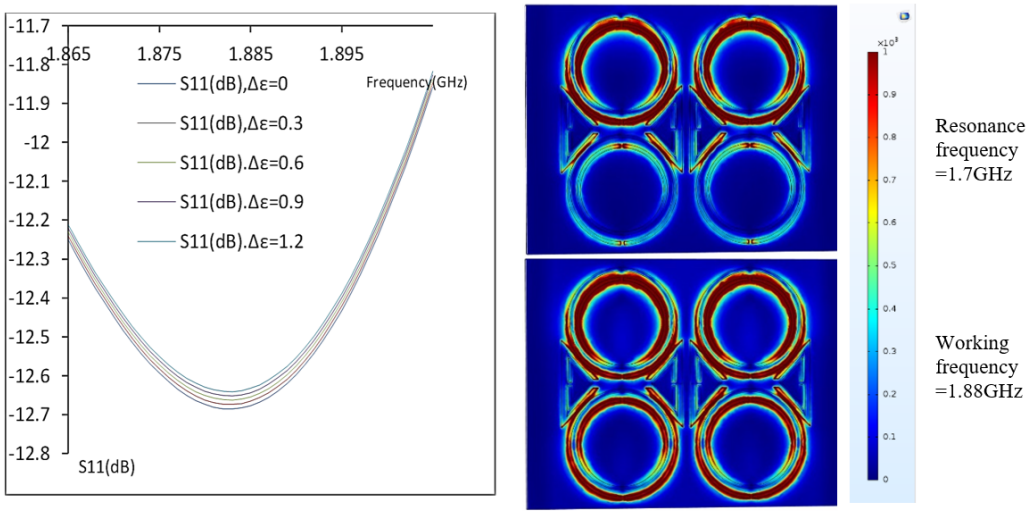

Figure 7: Simulation results of (a) S_{11} versus frequency for $\Delta\varepsilon$=0.02, (b) Electric field distribution on the resonator at the frequency of 1.88 GHz and 1.7GHz for $\Delta\varepsilon$=0

In Fig. 7b, the distribution of electric fields is represented by different colors; the displayed distribution is performed at the resonator level. The dark red color has the maximum electric field intensity, which corresponds to a value of 1000 V/m based on the simulation. The lumped port attribute used in feeding the coplanar line is the uniform element of port 2 with an excitation wave voltage equal to 0.2V.The selection of the working frequency is made according to the effect of glucose on the water permittivity, in fact, glucose has a very weak effect in high frequencies [36]. On the other hand, working at very low frequencies results in high sensor size values. A compromise must be made between sensor size and sensitivity to glucose. The optimal operating frequency is found at the $|S11|_{dB}$ lower peak in this type of configuration. Indeed, by comparing to the lower peak of $|S21]_{dB}$ at the resonance frequency 1.7GHz, there are only the first two SRRs that generate a strong electric field to interact with the study medium (the study medium in the case of this study is water). The optimal frequency is chosen at 1.88GHz so that the electric field distribution on the sensor is similar over the four SRRs.(see Figure 7(b)) . The intensity of the electric field has also been observed to be high in the gap between the rings and the adjacent triangles, due to the capacities effect that was created.

Fig. 8 presents the electric field norm in water. The maximum value of the electric field is 30 V/m, which is indicated by the dark red color. A sudden drop-off in the electric field was observed at the separation interface between the insulator and the water. This can be explained by the significant difference in permittivity between the insulator and the water.

To visualize the attenuation of the electric field E as a function of the depth in the water, this study proposes an electric field norm inside the water block. The electric field E was above 800 V/m before the interface that separated the insulator from the water. In Fig. 8b,

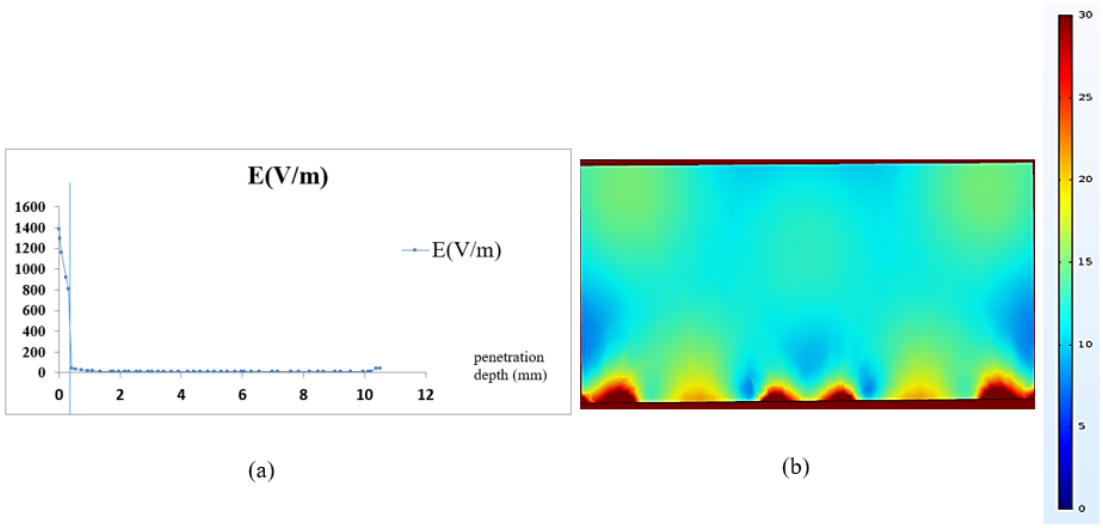

Figure 8: (a) electric field versus (Penetration Depth), (b) The electric field distribution (V/m) in the water

at the interface between the insulator and the water, the electric field drops from 800 V/m in the insulator at maximum electric field to 42.77 V/m in glucose water. As the electric field is highly concentrated in the bottom of the sample, it is expected that small variations in the filling volume have very small influence in the S11 magnitude.

Experimental study

An experimental study was carried out to validate the simulation results. First, the following steps are proposed to fabricate the sensor, and to select dimensions and materials. Then, the specific measurement protocol will be presented in detail. Finally, the results will be interpreted and discussed.

Materials

After modeling the antenna on COMSOL, a Gerber format file was generated to be inserted into the printed circuit board manufacturing equipment; the antenna was manufactured by subcontracting. The biosensor consists of ring and triangular resonators, which are fed by coplanar line that located on the second face of the substrate. The substrate used for the fabrication of antennas is the Rogers 3210, with a relative permittivity of 10.2 and a substrate thickness of 1.27 mm. In addition to being commercially available, this substrate allows a high coupling between the coplanar line and the resonator, as well as the optimal dimensions of the structure (resonator dimensions, distance between SMA pin connectors, which is 1.3 mm, etc.). However, the width of the central strip of the coplanar line was not suitable for the SMA size standard, which led us in adapting to the structure by adding a coplanar line/coplanar line transition (see Fig.9. a). The thickness of the copper used to etch the metal parts is 35 μm, and the size of the sensor is 56 $\times$ 30.6 mm^2.

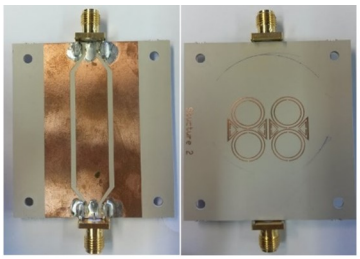

Figure 9: (a) First face of the antenna, (b) the second face of the antenna.

As shown in Fig. 9, in the photo (a), the SMA connectors were soldered to the coplanar line so as to enable the outer part of the SMA, representing the ground, to be connected to the ground plane of the coplanar line, and the central conductor of the SMAs was connected to the central strip of the coplanar line. Using a network analyzer, the coplanar line was fed through a coaxial cable with characteristic impedance equal to 50Ω. The magnetic field produced in the slot of the coplanar line can be expressed as a solenoidal vector field; the closed circular boundaries of the magnetic lines enclose the central strip of the coplanar line. Due to the change in the magnetic field, an induced current was generated in each of the spires of the resonator. The capacitiveeffect was created between each adjacent spire of the SRR due to the electric charges' distribution.

In Vitro test

Experimental measurements of glucose water were performed. Two coaxial cables were used to connect the antenna to the vector network analyzer (Agilent N5230A 300 KHz-20 GHz). Both cables were manufactured by Atem-RF & Microwave Company. Both cables operate at frequencies up to 18 GHz. The cables have an inner conductor diameter of 1.02 mm.

The measurement configuration consists of:

(a) A circular glass-shaped water holder placed on the face of the resonators, with a volume of 7.5 ml, a diameter of 32 mm, and a wall thickness of 0.5 mm.

b) The antenna to be tested.

c) A temperature sensor whose function is to measure the temperature of the medium and can detect a variation of 0.01°C.

d) Glucose powder.

The water holder was placed on the side carrying the resonator, and then was filled to a volume of 7.5 ml using a graduated pipette.

Prior to the start of the measurement, the VNA was calibrated based on the SOLT method (Short-Open-Load-Thru) using the 85033 D/E 3.5 mm kit. The frequency band was adjusted between 300 KHz and 3 GHz, which was sufficient to characterize the sensor that operates in the [1.5, 2.5] GHz range. On the other hand, the signal power emitted from the analyzer was set to -8 dBm.

External factors such as temperature, mechanical vibrations, and instrument errors can affect the accuracy of measurements, making errors in the measured value inevitable. Therefore, the result of each measurement will be the average of a set of samples collected within a well-defined time interval.

The measurements were performed by tracking the |S11| peak for different glucose concentration and evaluate its magnitude value. The measurement protocol followed is:

- The resonator was characterized with the holder filled with pure water, and the magnitude of S_{11} was read following system stability.

- 3.75 mg of glucose powder was then added to the water and the solution was mixed to homogenize water + glucose.

- Data acquisition of the S11 magnitude peak was performed.

- The same procedure was repeated by varying the glucose concentrations in the range of 1.7346 mmol/l to 13.87 mmol/l. This measurement protocol can effectively eliminate the reading error caused by using different micro pipettes to fill a sample holder with different aqueous glucose solutions. The molar mass of glucose is 180.156 g/mol, and the volume error in the water created by adding glucose is less than 0.03%.

At the beginning of the experiment, the water temperature was measured and considered constant during the experimental measurement. Certainly, the duration of each experimental measurement is less than 2 h, and the change introduced in the measured temperature ΔT is less than 0.5°C. For more details on the effect of temperature on the reflection coefficient S_{11}, this seems to be an acceptable error [15].

The slider on the network analyzer was adjusted to obtain information on the magnitude of S_{11} at various working frequencies. The choice of the working frequency is based on the resonance frequency of S_{21}. At this frequency, the resonators behave like a stop band filter. The first two resonators in the structure reacted like a short circuit; as a result, the second cell of SRR is inactive. That is why we chose to work at the minimum (reflect-mode) of the resonator response.

The second face of the antenna was placed in such a way that the water would be in direct contact with the resonators through the insulating layer of the holder. Then, 3.75 mg of glucose powder was added to the water every 10 min. This is equivalent to increasing the glucose concentration in 2.77 mmol/l steps. The magnitude of S_{11} was measured for each glucose concentration.

Results and discussion

Following the measurement method, two graphs of magnitude S_{11}, as shown in Fig. 10, were plotted at a frequency of 1.8 GHz and at room temperature between 29°C and 31.1°C.

At a temperature of 31.1°C, the curve has a slope of 0.0076 dB/(mmol/l), which is higher than that presented at a temperature of 29°C (0.0036dB/(mmol/l)). The two curves show a correlation of magnitude S_{11}, expressed in dB, with glucose concentration at the 1.8 GHz frequency. The estimated error sizes are comparable to the symbol size. The main error sources are the instrumental error in the VNA for the y-axis and the volume sampling error (roughly 0.03%) that can be introduced. The error in glucose concentration is 0.03% C_g for each coefficient, where C_g is the glucose concentration. Several measurements were made

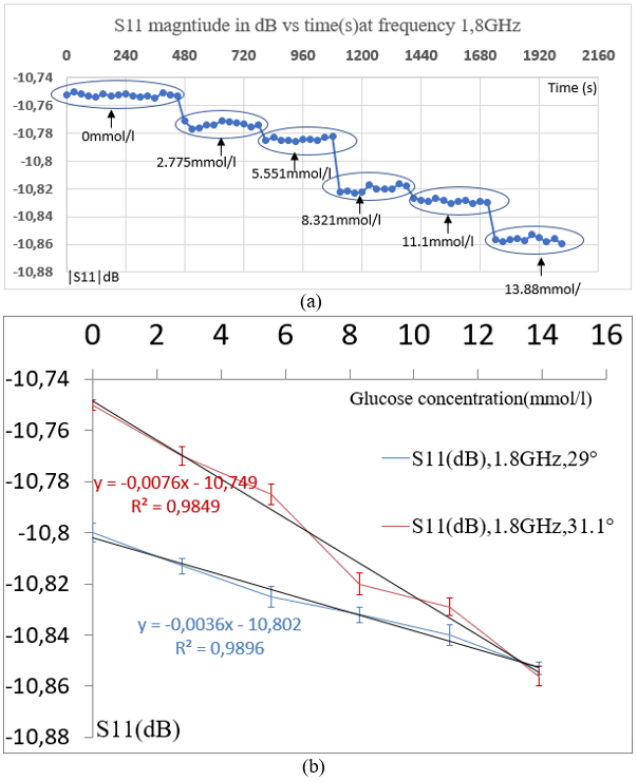

Figure 10: (a) |S11| versus time for different change in glucose concentration (b)S11 (dB) vs glucose concentration in the water, at a frequency of 1.8 GHz

at different frequencies, and optimal sensitivity was obtained at frequencies near the center frequency f_0. f_0 represents the frequency where the structure is matched to 50Ω. Estimation of the glucose concentration would have been possible if the frequency shift, quality factor, and other parameters had been chosen. In this paper, the focus is on the S_{11}reflected mode, which has led us to develop a simple electronic circuit based on the power detector circuit to quantify the reflected power according to glucose levels.

Study of glucose concentration using an electronic card

Developing an electronic card for acquiring signals from RF sensors is an important step for the realization of a non-invasive biosensor, considering the dimensions of the sensor and its electronic card. The schematic diagram is presented in Fig. 11.

The electronic acquisition system consists of:

-A VCO, which provides a Radio Frequency (RF) signal. The reference of the VCO used is CVCO55BE (1200-2300) MHz; its typical output power is 4dBm. The VCO output is an RF signal controlled by DC voltage generator at its input.

- The CF1724 circulator, which has an isolation of 20 dB and an insertion loss of 0.5dB in the 1.7-2.4 GHz frequency band.

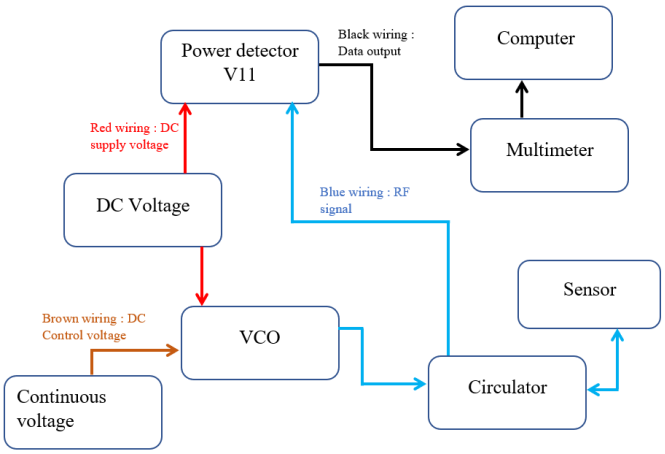

Figure 11: Hardware architecture synoptic scheme

- The used LTC5509 power detector operating at 300 MHz and 3 GHz. A temperature compensated Schottky diode peak detector and buffer amplifier are combined in a small SC70 package. The input power level operates in the range of -30 dBm to 6 dBm.

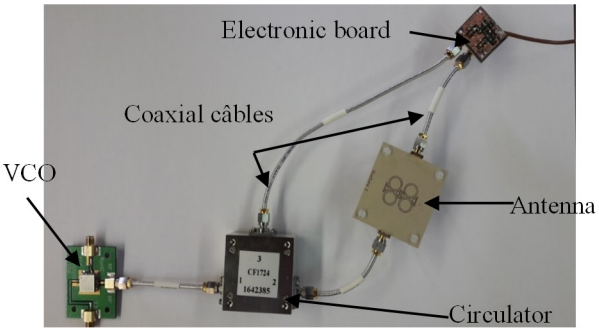

Figure 12: Full system of the sensor

The output voltage V_{11} of the power detector is transmitted through a multi meter connected to a computer using a GPIB card. GPIB is an interface used for communication between electronic measuring devices and a computer. The software programs developed in LabVIEW were used for data acquisition to monitor the glucose level in water in real time.

Measurement results are shown in Figure 13(b). The presented data points correspond to one test. The electronic readout stabilization is checked before starting the tests with glucose. The figure presents the obtained results for one test once the spikes in the output voltage, created by the use of a rod, have been suppressed. The acquisition of each point is made every 2 seconds. More than five hundred points are acquired for one defined glucose concentration, which corresponds to 20 minutes, this is enough to demonstrate the output voltage stabilization. At first, the initial output voltage was constant. When glucose was added, the output voltage decreased and stabilized after a short time. This reduction in output voltage occurs because of glucose.

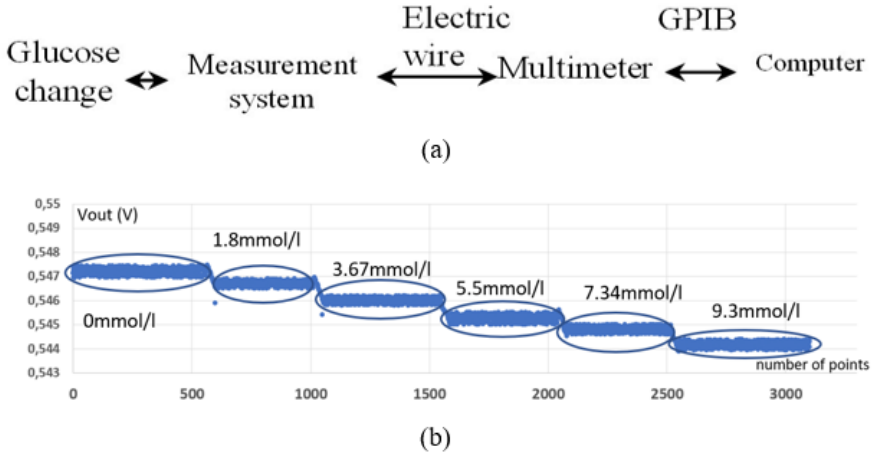

Figure 13: Voltage acquisition vs number of points using LabVIEW

Several measurements were made at different frequencies around 1.88 GHz. The same protocol measurement, as previously described, has been used. In the beginning, many tests were performed by gradually adding 5 mg after collecting many data points, which is equivalent to a change in glucose concentration of 3.33 mmol/l. Then, other tests were made to evaluate the smallest step the sensor can detect, the glucose concentration is increased by a step of 1.665mmol/l . Each data points presented in figure 14 and 15 are estimated using the average of 500 points:

$x_{mean} = \frac{\sum_1^n x_i}{n}$

The results obtained show the correlation between the voltage V_{11} and the concentration of glucose in water. The effect of glucose on permittivity is very low at 2.5 GHZ. A variation in glucose concentration from 4 mmol/l to 33.3 mmol/l results in a change in relative permittivity equal to 0.21.

In Fig. 14, Although the initial values of the voltage are different due to slight changes in the placement of the water holder between each test, thus, the experimental results show a good correlation between the sensor response and the glucose concentration in water at a defined position of the water holder. The linear tendency of the output voltage is almost the same for different tests. The slope in (mV/(mmol/l)) from test1 to test 4 is equal to -0.1, -0.2, -0.2, -0.2 respectively. The worst coefficient of determination between the 4 tests obtained was R^2equal to 0.9068.

In addition to the results shown in Figure 14, more measurements were made with the aim of seeing if small change in glucose concentrations at physiological levels could be detected. The results are shown in figure 15.

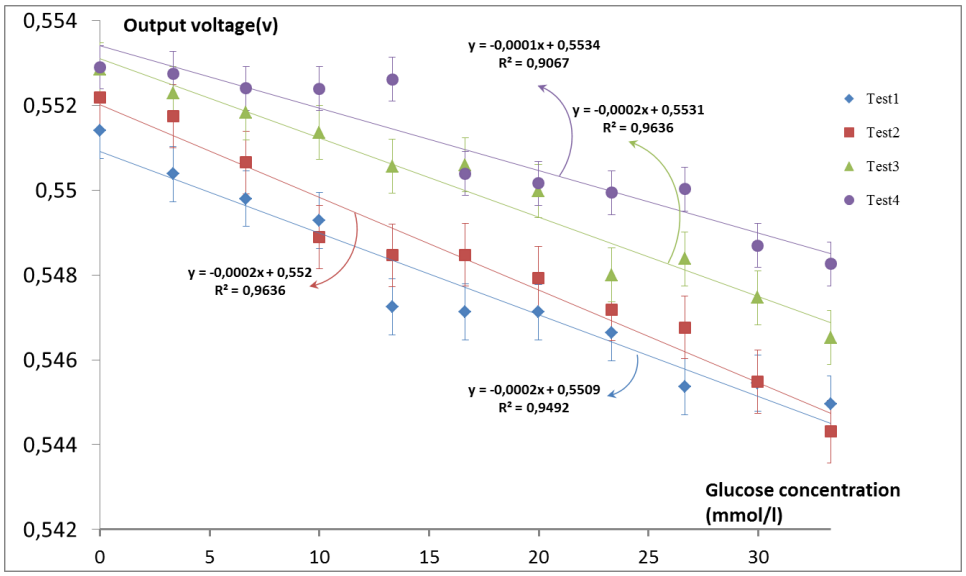

Figure 14: The output voltage V11 for different glucose concentrations (Reproductibility study)

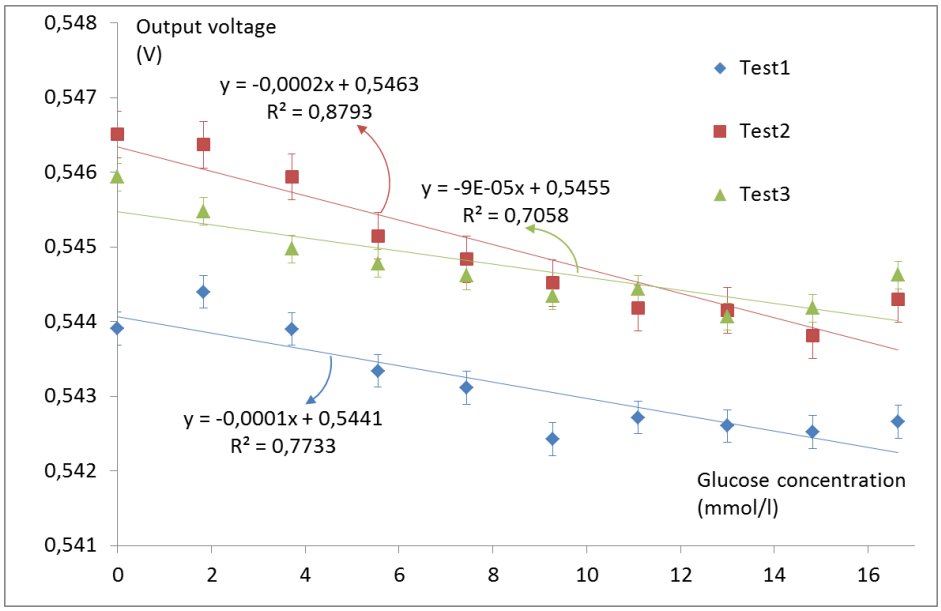

Figure 15: The output voltage V11 for different glucose concentrations (Resolution)

Comparative study

By using simulation, this study found a variation of S_{11} to be equal to 0.033 around -12.675dB for a variation step of $\Delta\varepsilon$, which is equal to 1.2 at the 1.9 GHz frequency. At the same frequency, the measurement results in the network analyzer show a variation of

S_{11} equal to 0.106 at around -10.8dB at 31.1°C and 0.053 at around -10.8dB for a variation in the glucose level between 0 mmol/l and13.877 mmol/l. This discrepancy between the simulation and the experiment is as a result of the simulation model not being able to consider certain physical parameters, such as temperature, water volume, and dimension of the insulating layer. In addition, the exact valuesof the variation in permittivity in water due to the glucose level cannot be precisely quantified by simulation, because the change in glucose has a weak impact on the relative permittivity of water, which makes it very difficult to quantify the variation in permittivity as a function of the glucose level. On the other hand, measurements on an electronic prototype produce a change in output voltage equal to 6.3 mV for a glucose concentration range between 0 mmol/l and 33.3 mmol/l and 2.3 mV for an interval ranging from 0 to 16.53 mmol/l. The results are shown in Table 1.

Table 1: Comparison of results between simulation and experience

Simulation	$\Delta\varepsilon = 1.2$	S11 = -12.675dB		ΔS11 = 0.033dB
Experimental measurement on (VNA) (1.88 GHz)	[0, 13.87] mmol/l	T = 31.1°C	S11 = -10.75dB	ΔS11 = 0.106dB
		T=29°C	S11 = -10.8dB	ΔS11 = 0.053dB
Electronic prototype (1.88 GHz)	[0, 33.30] mmol/l	Output voltage = 552 mV		ΔV = 6.3mV

In the state-of-the-art, several parameters related to the sensor have been used to improve the sensor sensitivity towards different glucose levels. Some of these parameters are reflection coefficient S_{11} [15] , transmission coefficient S_{21} [35, 37] and quality factor Q [37] , resonance frequency [38] , input impedance, and signal phase.

[21] uses a coplanar wave guide (CPW) loaded with a split ring resonator (SRR) for detecting aqueous sucrose solution with a step of 1100mmol/l, the used method consists in evaluating the S21 amplitude at the frequency range [2-3] GHz. The sensor shows a high dynamic range and linearity. However, smaller concentrations have not been investigated. [35]uses an inter digital capacitor, the sensor shows a lack of sensitivity for smaller glucose concentration lower than 30 mmol/l. The sensing in [37]is based in two port |S21| and using quality factor for measuring glucose. Three version of the sensor are studied between 2GHz and 7GHz, good sensitivity has been obtained compared with some other works in the state of art. In [38], a complementary electric-LC resonator coupled with a microstrip line is designed to operate between [1.2GHz,1.4GHz], it is shown that by flowing water-glucose solution to the sensing area, the resonance property of the resonator is modified, this measurable change in the electromagnetic property is then used to quantify the glucose concentration. The device in [39] is based on a splitter/combiner microstrip structure loaded with a pair of split ring resonators (SRRs) in a symmetric configuration, it

is demonstrated that glucose as small as 5.5 mmol/l can be measured.

The readout electronic is an important aspect to consider. Indeed, the most part of the work, cited in the state of art, use a VNA for measuring glucose. However, the resolution and the sensitivity can be improved by providing a suitable electronics which can implement signal processing algorithms, therefore, it helps to reduce the noise and estimate efficiently a measurement parameter.

Table 2: Comparison with previous studies

Ref.	The used parameter	Frequency	Sensitivity
[21]	S21	2.44 GHz	0.000884 dB/(mmol/l)
[35]	S11	[4 GHz-5 GHz]	Lack of sensitivity for glucose concentration lower than 30mmol/l
[37]	Q, S21	1.92 GHz, 5.16 GHz, 7.16 GHz	Good sensitivity, but not convenient because a microliter volume of water is used in a restraint area.
[38]	S21	[1.2GHz-1.4GHz]	0.08525MHz/(mmol/l)
[39]	S21	[746MHz-758MHz]	0.0099dB/(mmol/l)
This work	S11	1.8 GHz 1.9 GHz	Using VNA: 0.0076dB/(mmol/l) Using electronic prototype: 0.2mV/(mmol/l)

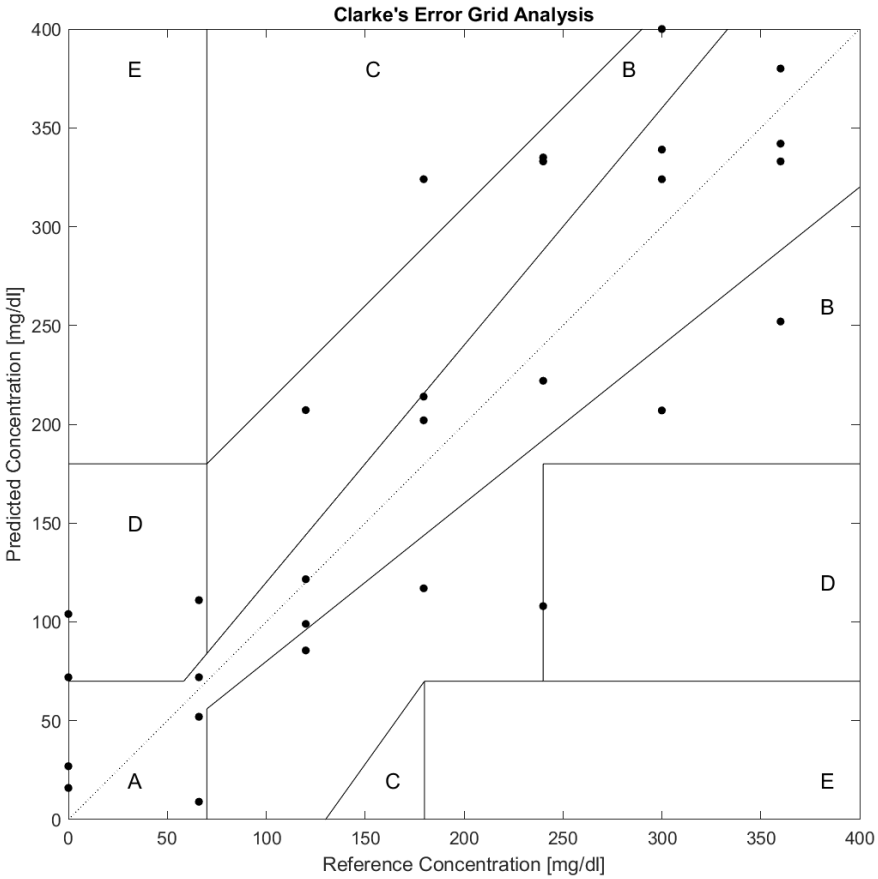

Figure 16: Clarke's error grid obtained by using the previous experimental results

For evaluating the biosensor reliability for hyperglycemia monitoring applications, the measured glucose concentrations are presented on Clarke error grid versus the actual concentration values. This grid is developed by Clarke on 1987 to quantify the clinical accuracy of the methods and systems in monitoring the blood glucose level [40] .

53.57 % of data points are located in Zone A (acceptable): it represents the glucose values that deviate from the reference values by $\pm 20\%$.

28.57% are located in Zone B (benign errors); this zone represents those values that deviate from the reference values, which are incremented by 20%. The values that fall within zones A and B are acceptable.

Conclusion

This paper presents a new type of microwave sensitive sensor for the non-invasive measurement of glucose in water. The detection side is composed of two cells of the circular split ring resonator (SRR) and four triangular SRRs. Introducing a change in glucose concentration in water modifies the sensor input impedance therefore the reflected coefficient |S11|. The sensor, used as glucose trackers, has been simulated and tested experimentally by VNA. Then, using an electronic prototype which is capable of reproducible detecting glucose concentration ranging from 0 to 560mmol/l by a step of 3.33 mmol/l. Its output voltage resolution is 0.2mV. The sensor is used for measuring the glucose concentration down to the physiological levels and interpretation of the measured results on Clarke grid demonstrates its potential for the blood glucose monitoring.

Acknowledgements

This work was supported by Region Grande-EST and FEDER

References

[1] J. Sheen, Comparisons of microwave dielectric property measurements by transmission/reflection techniques and resonance techniques, Measurement Science and Technology 20 (4) (2009) 042001–042001. doi:10.1088/0957-0233/20/4/042001.
URL https://dx.doi.org/10.1088/0957-0233/20/4/042001

[2] S. S. Stuchly, C. E. Bassey, Microwave coplanar sensors for dielectric measurements, Measurement Science and Technology 9 (8) (1998) 1324–1329. doi:10.1088/0957-0233/9/8/027.
URL https://dx.doi.org/10.1088/0957-0233/9/8/027

[3] D. Khaled, N. Novas, J. Gazquez, R. Garcia, F. Manzano-Agugliaro, Fruit and Vegetable Quality Assessment via Dielectric Sensing, Sensors 15 (7) (2015) 15363–15397. doi:10.3390/s150715363.
URL https://dx.doi.org/10.3390/s150715363

[4] T. Gaspard, A. Cuevas, I. Cuiñas, I. Expósito, J. Verhaevert, Electromagnetic characterization of cola drinks, Measurement 107 (2017) 111–119. doi:10.1016/j.measurement.2017.05.018.
URL https://dx.doi.org/10.1016/j.measurement.2017.05.018

[5] A. Ebrahimi, F. J. Tovar-Lopez, J. Scott, K. Ghorbani, Differential Microwave Sensor for Characterization of Glycerol-Water Solutions, Sensors and Actuators B: Chemical 321 (128561) (2020).

[6] J. Venkataraman, B. Freer, Feasibility of non-invasive blood glucose monitoring: In-vitro measurements and phantom models, in: 2011 IEEE International Symposium on Antennas and Propagation (APSURSI), 2011, pp. 603–606.

[7] G. Gennarelli, S. Romeo, M. R. Scarfi, F. Soldovieri, A Microwave Resonant Sensor for Concentration Measurements of Liquid Solutions, IEEE Sensors Journal 13 (5) (2013) 1857–1864. doi:10.1109/jsen.2013.2244035.
URL https://dx.doi.org/10.1109/jsen.2013.2244035

[8] E. N. Shaforost, N. Klein, S. A. Vitusevich, A. A. Barannik, N. T. Cherpak, High sensitivity microwave characterization of organic molecule solutions of nanoliter volume, Applied Physics Letters 94 (11) (2009) 112901–112901. doi:10.1063/1.3097015.
URL https://dx.doi.org/10.1063/1.3097015

[9] T. Yilmaz, R. Foster, Y. Hao, Radio-Frequency and Microwave Techniques for Non-Invasive Measurement of Blood Glucose Levels, Diagnostics 9 (1) (2019) 6–6. doi:10.3390/diagnostics9010006.
URL https://dx.doi.org/10.3390/diagnostics9010006

[10] E. C. Green, Design of a Microwave Sensor for Non-Invasive Determination of Blood-Glucose Concentration (2005).
[11] . US Patent 5, 119, Method and apparatus for non-invasive monitoring of blood glucose (1992).
[12] S. Kim, H. Melikyan, J. Kim, A. Babajanyan, J.-H. Lee, L. Enkhtur, B. Friedman, K. Lee, Noninvasive in vitro measurement of pig-blood d-glucose by using a microwave cavity sensor, Diabetes Research and Clinical Practice 96 (3) (2012) 379–384. doi:10.1016/j.diabres.2012.01.018.
URL https://dx.doi.org/10.1016/j.diabres.2012.01.018
[13] S. Harnsoongnoen, A. Wanthong, Coplanar Waveguide Transmission Line Loaded With Electric-LC Resonator for Determination of Glucose Concentration Sensing, IEEE Sensors Journal 17 (6) (2017) 1635–1640. doi:10.1109/jsen.2017.2652121.
URL https://dx.doi.org/10.1109/jsen.2017.2652121
[14] H. Choi, Design and In Vitro Interference Test of Microwave Noninvasive Blood Glucose Monitoring Sensor, IEEE Transactions on Microwave Theory and Techniques 63 (2015) 3016–3025.
[15] K. Lee, A. Babajanyan, C. Kim, S. Kim, B. Friedman, Glucose aqueous solution sensing by a near-field microwave microprobe, Sensors and Actuators A: Physical 148 (1) (2008) 28–32. doi:10.1016/j.sna.2008.06.024.
URL https://dx.doi.org/10.1016/j.sna.2008.06.024
[16] B. M, A. Z. and Daneshmand M, L. PE, Non-invasive continuous-time glucose monitoring system using a chipless printable sensor based on split ring microwave resonators, Sci Rep (2020). doi:10.1038/s41598-020-69547-1.
URL https://pubmed.ncbi.nlm.nih.gov/32737348/
[17] L. Guadarrama-Fernández, M. Novell, P. Blondeau, F. J. Andrade, A disposable, simple, fast and low-cost paper-based biosensor and its application to the determination of glucose in commercial orange juices, Food Chemistry 265 (2018) 64–69. doi:10.1016/j.foodchem.2018.05.082.
URL https://dx.doi.org/10.1016/j.foodchem.2018.05.082
[18] A. L. Galant, R. C. Kaufman, J. D. Wilson, Glucose: Detection and analysis, Food Chemistry 188 (2015) 149–160. doi:10.1016/j.foodchem.2015.04.071.
URL https://dx.doi.org/10.1016/j.foodchem.2015.04.071
[19] J. Naqui, L. Su, J. Mata, F. Martín, Recent Advances in the Modeling of Transmission Lines Loaded with Split Ring Resonators, International Journal of Antennas and Propagation 2015 (2015) 1–13. doi:10.1155/2015/792750.
URL https://dx.doi.org/10.1155/2015/792750
[20] F. Aznar, M. Gil, J. Bonache, F. Martín, Modelling metamaterial transmission lines: a review and recent developments, Opto-Electronics Review 16 (3) (2008) 226–236. doi:10.2478/s11772-008-0028-x.
URL https://dx.doi.org/10.2478/s11772-008-0028-x
[21] S. Harnsoongnoen, A. Wanthong, Coplanar waveguides loaded with a split ring resonator-based microwave sensor for aqueous sucrose solutions, Measurement Science and Technology 27 (1) (2016) 015103–015103. doi:10.1088/0957-0233/27/1/015103.
URL https://dx.doi.org/10.1088/0957-0233/27/1/015103
[22] M. Wellenzohn, M. Brandl, A Theoretical Design of a Biosensor Device Based on Split Ring Resonators for Operation in the Microwave Regime (2015). doi:10.1016/j.proeng.2015.08.737.
URL https://dx.doi.org/10.1016/j.proeng.2015.08.737
[23] D. Sathyanath, M. P. Jayakrishnan, T. H. P, S. Mridula, P. Mohanan, Microwave Based Biosensor for Blood Glucose Monitoring, in: 2015 Fifth International Conference on Advances in Computing and Communications (ICACC), 2015, pp. 362–365.
[24] L. Su, J. Naqui, J. Mata-Contreras, F. Martin, Modeling Metamaterial Transmission Lines Loaded With Pairs of Coupled Split-Ring Resonators, IEEE Antennas and Wireless Propagation Letters 14 (2015) 68–71. doi:10.1109/lawp.2014.2355035.
URL https://dx.doi.org/10.1109/lawp.2014.2355035
[25] P. A. Hasgall, F. D. Gennaro, C. Baumgartner, E. Neufeld, B. Lloyd, M. C. Gosselin, D. Payne, A. Klingenböck, N. Kuster (2018).

[26] T. Karacolak, E. C. Moreland, E. Topsakal, Cole-cole model for glucose-dependent dielectric properties of blood plasma for continuous glucose monitoring, Microwave and Optical Technology Letters 55 (5) (2013) 1160–1164. doi:10.1002/mop.27515.
URL https://dx.doi.org/10.1002/mop.27515

[27] P. Vélez, K. Grenier, J. Mata-Contreras, D. Dubuc, F. Martín, Highly-Sensitive Microwave Sensors Based on Open Complementary Split Ring Resonators (OCSRRs) for Dielectric Characterization and Solute Concentration Measurement in Liquids, IEEE Access 6 (2018) 48324–48338. doi:10.1109/ACCESS.2018.2867077.

[28] L. Su, J. Mata-Contreras, P. Vélez, A. Fernández-Prieto, F. Martín, Analytical Method to Estimate the Complex Permittivity of Oil Samples, Sensors 18 (4) (2018) 984–984. doi:10.3390/s18040984.
URL https://dx.doi.org/10.3390/s18040984

[29] P. Vélez, J. Muñoz-Enano, K. Grenier, J. Mata-Contreras, D. Dubuc, F. Martín, Split Ring Resonator-Based Microwave Fluidic Sensors for Electrolyte Concentration Measurements, IEEE Sensors Journal 19 (7) (2019) 2562–2569. doi:10.1109/JSEN.2018.2890089.

[30] A. Ebrahimi, W. Withayachumnankul, S. Al-Sarawi, D. Abbott, High-Sensitivity Metamaterial-Inspired Sensor for Microfluidic Dielectric Characterization, IEEE Sensors Journal 14 (5) (2014) 1345–1351. doi:10.1109/jsen.2013.2295312.
URL https://dx.doi.org/10.1109/jsen.2013.2295312

[31] A. Ebrahimi, J. Scott, K. Ghorbani, Microwave reflective biosensor for glucose level detection in aqueous solutions, Sensors and Actuators A: Physical 301 (2020) 111662. doi:https://doi.org/10.1016/j.sna.2019.111662.

[32] A. Ebrahimi, J. Scott, K. Ghorbani, Ultrahigh-Sensitivity Microwave Sensor for Microfluidic Complex Permittivity Measurement, IEEE Transactions on Microwave Theory and Techniques 67 (10) (2019) 4269–4277. doi:10.1109/TMTT.2019.2932737.

[33] N. Sharafadinzadeh, M. Abdolrazzaghi, M. Daneshmand, Investigation on planar microwave sensors with enhanced sensitivity from microfluidic integration, Sensors and Actuators A: Physical 301 (2020) 111752. doi:https://doi.org/10.1016/j.sna.2019.111752.

[34] M. Wellenzohn, M. Brandl, A Theoretical Design of a Biosensor Device Based on Split Ring Resonators for Operation in the Microwave Regime, Procedia Engineering 120 (2015) 865–869. doi:10.1016/j.proeng.2015.08.737.
URL https://dx.doi.org/10.1016/j.proeng.2015.08.737

[35] V. Turgul, I. Kale, Characterization of the complex permittivity of glucose/water solutions for non-invasive RF/Microwave blood glucose sensing, IEEE International Instrumentation and Measurement Technology Conference Proceedings (2016) 1–5.

[36] P. F. M. Smulders, M. G. Buysse, M. D. Huang, Dielectric Properties of Glucose Solutions in the 0.5–67 GHz Range, Microwave and Optical Technology Letters 55 (8) (2013) 1916–1917. doi:https://doi.org/10.1002/mop.27672.

[37] C. G. Juan, E. Bronchalo, B. Potelon, C. Quendo, E. Avila-Navarro, J. M. Sabater-Navarro, Concentration Measurement of Microliter-Volume Water–Glucose Solutions Using Q Factor of Microwave Sensors, IEEE Transactions on Instrumentation and Measurement 68 (7) (2019) 2621–2634. doi:10.1109/tim.2018.2866743.
URL https://dx.doi.org/10.1109/tim.2018.2866743

[38] A. Ebrahimi, W. Withayachumnankul, S. F. Al-Sarawi, D. Abbott, Microwave microfluidic sensor for determination of glucose concentration in water, in: 2015 IEEE 15th Mediterranean Microwave Symposium (MMS), 2015, pp. 1–3. doi:10.1109/MMS.2015.7375441.

[39] P. Vélez, J. Mata-Contreras, D. Dubuc, K. Grenier, F. Martín, Solute Concentration Measurements in Diluted Solutions by means of Split Ring Resonators, in: Proc. 48th Europ. Microw. Conf, 23-28 Sep. 2018, Madrid.

[40] W. L. Clarke, D. Cox, L. A. Gonder-Frederick, W. Carter, S. L. Pohl, Evaluating Clinical Accuracy of Systems for Self-Monitoring of Blood Glucose (1987). doi:10.2337/diacare.10.5.622.
URL https://dx.doi.org/10.2337/diacare.10.5.622

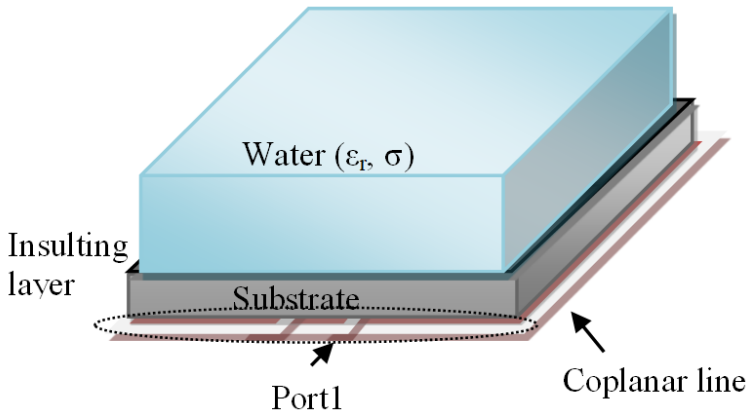

It’s still challenging to measure glucose in liquid using non invasive sensor. Four planar resonators are designed to improve the electromagnetics interactions between the sensor and the medium being studied. A resolution of 1,665mmol/l is reached using a proposed measurement system.

Glucose change ↔ Measurement system ↔ (Electric wire) Multimeter ↔ (GPIB) Computer →